AD-A035 726 ROCKWELL INTERNATIONAL THOUSAND OAKS CALIF SCIENCE --ETC F/G 7/4
EFFECT OF CAVITY LOADING ON ANALYTICAL ELECTRON SPIN RESONANCE --ETC(U)
FEB 77 I B GOLDBERG, H R CROWE N00014-73-C-0325

UNCLASSIFIED SC549.22TR NL

1 OF 1
AD A035726

END

DATE FILMED
3-77

SC549.22TR February 1977

EFFECT OF CAVITY LOADING ON ANALYTICAL ELECTRON SPIN RESONANCE SPECTROMETRY

Technical Report No. 8

Covering the Period Oct. 1, 1976 to Jan. 31, 1977

Contract No. N00014-73-C-0325
Task No. NR051-553

Prepared for

Office of Naval Research
Arlington, VA 22217

by

Ira B. Goldberg
Harry R. Crowe

Approved for public release; distribution unlimited.

Science Center
Rockwell International
1049 CAMINO DOS RIOS
THOUSAND OAKS, CALIF. 91360
805/498 4545

UNCLASSIFIED

SECURITY CLASSIFICATION OF THIS PAGE (When Data Entered)

REPORT DOCUMENTATION PAGE

READ INSTRUCTIONS BEFORE COMPLETING FORM

1. REPORT NUMBER (on)

2. GOVT ACCESSION NO.

3. RECIPIENT'S CATALOG NUMBER

4. TITLE (and Subtitle) (6)
Effect of Cavity Loading in Analytical Electron Spin Resonance Spectrometry.

5. TYPE OF REPORT & PERIOD COVERED
Technical Report
10/01/76 to 1/31/77

6. PERFORMING ORG. REPORT NUMBER (14)
SC549.22TR

7. AUTHOR(s) (10)
Ira B. Goldberg [redacted] Harry R. Crowe

8. CONTRACT OR GRANT NUMBER(s) (15)
N00014-73-C-0325

9. PERFORMING ORGANIZATION NAME AND ADDRESS
Science Center
Rockwell International
Thousand Oaks, CA 91360

10. PROGRAM ELEMENT, PROJECT, TASK AREA & WORK UNIT NUMBERS
NR051-553

11. CONTROLLING OFFICE NAME AND ADDRESS
Materials Sciences Division
Office of Naval Research
Arlington, VA 22217

12. REPORT DATE (11)
Feb [redacted] 77

13. NUMBER OF PAGES (12) 25 p.
22

14. MONITORING AGENCY NAME & ADDRESS (if different from Controlling Office)
Office of Naval Research, Branch Office
1030 East Green Street
Pasadena, CA 91106

15. SECURITY CLASS. (of this report)
Unclassified

15a. DECLASSIFICATION/DOWNGRADING SCHEDULE

16. DISTRIBUTION STATEMENT (of this Report)
Approved for public release; distribution unlimited

17. DISTRIBUTION STATEMENT (of the abstract entered in Block 20, if different from Report) (9)
Technical rept. no. 8, 1 Oct 76-31 Jan 77.

18. SUPPLEMENTARY NOTES
To be submitted to Analytical Chemistry

19. KEY WORDS (Continue on reverse side if necessary and identify by block number)

Electron Paramagnetic Resonance
Electron Spin Resonance
Chemical Analysis
Manganese Sulfate
Diphenylpicrylhydrazyl
Standardization

20. ABSTRACT (Continue on reverse side if necessary and identify by block number)

The effect of cavity loading during magnetic resonance absorption on the accuracy of analysis by electron spin resonance techniques is calculated. Large samples, which degrade the cavity Q-factor due to absorption of a large fraction of the incident radiation cause a non-linearity of the absorption as a function of concentration. This is reflected by a broadening of the first derivative spectrum and reductions of the peak-to-peak amplitude and the double integral of the derivative from that predicted on the basis of diluted sample. → next page

DD FORM 1 JAN 73 1473 EDITION OF 1 NOV 65 IS OBSOLETE 389 949

UNCLASSIFIED

SECURITY CLASSIFICATION OF THIS PAGE (When Data Entered)

Calculations of this effect are verified with samples of $MnSO_4 \cdot H_2O$. Non-linearities in the order of 1% may be obtained with samples of 0.4 to 1.0 mg of $MnSO_4 \cdot H_2O$ or 0.1 to 0.25 mg of diphenylpicrylhydiazyl (DPPH) which are commonly used standards.

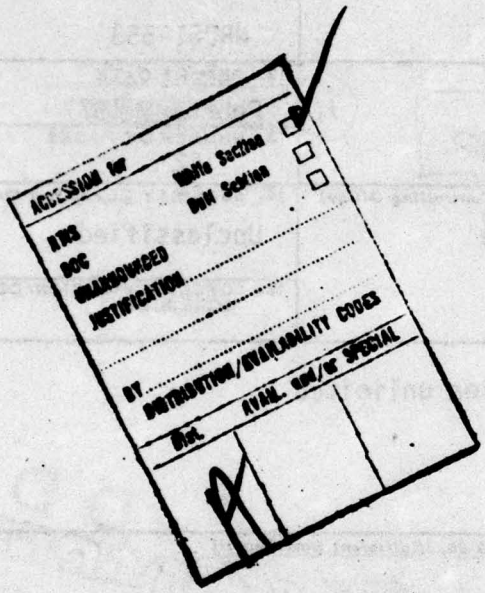

BRIEF

The effect of sample size on the analytical accuracy of electron spin resonance is discussed. Cavity loading effects cause a non-linearity of the response for intense samples. Maximum sample sizes are about 0.4 to 1 mg of $MnSO_4 \cdot H_2O$ or 0.1 to 0.25 mg of diphenylpicrylhydrazyl for 1% deviations from linearity. The nature of the sample and esr cavity determine the maximum quantity that should be used. The peak to peak amplitude is more strongly influenced than double integral values.

ABSTRACT

The effect of cavity loading during magnetic resonance absorption on the accuracy of analysis by electron spin resonance is calculated. Large samples which degrade the cavity Q-factor due to absorption of a large fraction of the incident radiation cause a non-linearity of the absorption as a function of the quantity of material. This is reflected by a broadening of the first derivative spectrum and reductions of the peak-to-peak amplitude and double integral of the ESR signal from that predicted on the basis of a dilute sample. The consequence of this effect is to underestimate the quantity of sample. Calculations of this effect were verified with samples of $MnSO_4 \cdot H_2O$. Non-linearities in the order of 1% may be obtained with samples of 0.4 to 1.0 mg of $MnSO_4 \cdot H_2O$ or 0.1 to 0.25 mg of diphenylpicrylhydrazyl which are commonly used standards for ESR.

INTRODUCTION

Electron spin resonance (ESR) derives much of its value from its high sensitivity and resolution. Hence, it is often used in the identification and quantification of trace impurities (1). However, there are many situations in which ESR can be used to quantitatively measure materials which exhibit intense paramagnetic absorption. Examples of this case include the calibration of ESR spectrometers, the analysis of fine grained iron in Lunar return samples (2), the determination of initial atom concentrations in studies of gas phase kinetics (3), the analysis concentrated solutions of radical ions or transition metal ions, and the separation and quantification of solid materials in mixtures by virtue of their unique temperature dependencies such as antiferromagnetic-paramagnetic transitions (4). While much attention has been devoted to the high sensitivity feature of ESR (5), the effect of the variation of the cavity Q-factor across the magnetic resonance has only been studied in terms of its effect on increasing the apparent linewidth of spectra (6).

We report here the effect of intense paramagnetic resonance absorption on the various parameters used in analysis. These include the peak-to-peak amplitude of the derivative of the absorption, the double integral of the first derivative, and the peak-to-peak amplitude multiplied by the square of the peak-to-peak linewidth. Both lorentzian and gaussian lineshapes are treated, and experimental data is presented.

EXPERIMENTAL

The ESR-computer system has been described in detail (7). It consists

of a modified V-4502 (Varian) ESR spectrometer with a Magnion 38 cm magnet and a PDP 8/m computer with 32 K words of core storage. Data was collected from the ESR spectrometer using a Basic program with assembly language functions for control of the multiplexor, analog to digital converter (ADC), clock, and other peripheral equipment. Two output registers control the upfield or downfield sweep direction, and the starting or stopping of the magnetic field sweep. A power meter was used to monitor the incident power to the cavity.

$MnSO_4 \cdot H_2O$ (Malinkrodt reagent grade) was recrystallized from water at 80°C and dried under N_2 for 48 hours. Heating two samples at 325°C for sixteen hours showed a 10.62% weight loss as compared to 10.66% theoretical. The ESR linewidth of this sample is 200 G, peak-to-peak. Each spectrum contained 1536 points, with 44 points between derivative extrema. Samples were weighed to $\pm$ 0.05 mg.

Integration of the spectra was carried out subsequent to the data acquisition. The intensity of each spectrum was between 70-100% of the full scale output of the ADC. Since the ADC is 12 bits, it is necessary to minimize numerical round-off errors.

Theoretical calculations of the effect of loading of the ESR cavity were also carried out using the PDP 8/m computer. Integrals of the absorption were computed to within $\pm$ 0.0002% by Simpson's rule. Derivatives were calculated from the computed absoprtion by finite differences. Due to the finite word size, accuracy was limited to $\pm$0.001 in the relative peak-to-peak width and $\pm$0.0002 in the relative peak-to-peak amplitudes.

THEORY

Cavity Q variation during resonance. The Q-factor of the microwave cavity during resonance, Q is related to its Q-factor off resonance, Q_o, and to the Q-factor of the sample Q_s, according to Eq. 1.

$$\frac{1}{Q} = \frac{1}{Q_o} + \frac{1}{Q_s} \tag{1}$$

Q_o is the Q-factor of the microwave cavity containing the paramagnetic sample and sample holder, but in which the magnetic field is such that there is no significant interaction of the magnetization of the sample with the incident radiation. The microwave loss caused by the sample magnetization in the ESR cavity is due entirely to its susceptibility, χ'', and to the filling factor, η, of the sample within the cavity (8). In cgs units,

$$\frac{1}{Q_s} = 4\pi\eta\chi'' \tag{2}$$

The filling factor is defined as the integral of the square of the microwave magnetic field, H_1^2 over the sample to that in the entire cavity

$$\eta = \left(\int_{sample} H_1^2 dv\right) \Big/ \left(\int_{cavity} H_1^2 dv\right) \tag{3}$$

Filling factors of rectangular and cylindrical cavities containing a variety of sample geometries have been calculated by Poole (8). These and several other cases are presented in Table I. The filling factor can be treated as being proportional to a constant, κ, times the ratio of the sample volume V_s to the cavity volume V_c,

$$\eta = \kappa \frac{V_s}{V_c}$$

The microwave susceptibility for the case in which the field is held constant and the frequency is swept is given by Eq. 5 (9),

$$\chi'' = \frac{1}{2}\omega_0\chi_0 \frac{T_2}{1 + (\omega-\omega_0)^2T_2^2} \tag{5}$$

where ω and ω_0 are the incident and resonant frequencies, and χ_0 is the static magnetic susceptibility. We assume that the line is not saturated by the level of incident radiation. For a paramagnetic material,

$$\chi_0 = \frac{g^2\beta^2 (S)(S+1) N,}{3k(T-\theta)V_s} \tag{6}$$

where N is the number of paramagnetic centers, S is the electron spin, g is the spectroscopic splitting factor, β is the Bohr magneton, k is the Boltzmann constant, T is the absolute temperature, and θ is the paramagnetic Curie temperature. The term $\eta\chi''$ is therefore proportional to the number of paramagnetic sites in the sample.

Equations 1 and 2 can now be rearranged to give

$$\frac{Q-Q_0}{Q_0} = \frac{\Delta Q}{Q_0} = \frac{4\pi\chi''Q_0\eta}{1+4\pi\chi''Q_0\eta} \tag{7}$$

Since the ratio of the absorbed power to the incident power is dependent on $\Delta Q/Q_0$, non-linearities in the response to the microwave susceptibility can result if $4\pi\chi''\eta Q_0$ is not negligible compared to unity. There are two consequences of this condition. The first is simply a saturation of $\Delta Q/Q_0$ due to an increase in the denominator of Eq. 7. This is of primary interest here. The second effect is caused by the non-linear response of the microwave detector to large changes in microwave power. Both of these effects

can lead to distortions of the lineshape.

RESULTS AND DISCUSSION

Lorentzian lineshape. Since Eq. 6 is not useful for typical analytical purposes, it can be converted to the conventional case of a fixed frequency of incident microwave radiation and a variable magnetic field, Eq. 8,

$$\chi'' = \frac{1}{\sqrt{3}} \chi_o H_o \frac{1}{\Delta_o} \frac{\Gamma^2}{\Gamma^2 + (H-H_o)^2} \tag{8}$$

where the halfwidth at one half of the maximum height of the absorption, Γ, is given by $\hbar/(T_2 g\beta)$, and the magnetic field H is given by $\hbar\omega/(g\beta)$. The peak-to-peak width, Δ_o, is equal to $2/\sqrt{3}\ \Gamma$. The maximum value of χ'' occurs when $H = H_o$. Thus the term $\eta Q_o \chi''_{max}$ where

$$\chi''_{max} = \frac{1}{\sqrt{3}} \chi_o\ H_o \frac{1}{\Delta_o} \tag{9}$$

is dependent on the nature and number of spins in the sample and on the parameters of the ESR cavity, and can be used to characterize the performance of the loaded cavity. The parameter $\eta Q_o \chi''_{max}$ is given by Eq. 10.

$$\eta Q_o \chi''_{max} = \kappa Q_o \frac{H_o}{\sqrt{3}\ \Delta_o} \cdot \frac{g^2\beta^2 S(S+1)N}{3V_c k(T-\theta)} \tag{10}$$

In order to compute the relative analytical parameters, $\Delta Q/Q_o$ was calculated from Eqs. 7 and 8 as a function of $4\pi\eta Q_o \chi''_{max}$. The relative analytical parameter is the value of the computed parameter, eg. peak-to-peak amplitude or double integral of the derivative spectrum, divided by the value of the parameter if $4\pi\eta\chi''_{max}\ Q_o \ll 1$. The values of those parameters which could be used for routine analysis are given as a function of the

Deciding upon the appropriate parameter to be used in analysis by ESR methods, the precision with which each term can be measured must be considered. For small quantities of paramagnetic material, in which intrinsic broadening due to the chemical exchange processes does not occur, the peak-to-peak amplitude is often the most convenient. At higher concentrations, however, this parameter is most greatly affected by cavity loading. Measurements of the peak-to-peak width are not precise, precluding $A \cdot \Delta^2$ as a suitable analytical parameter. Also, if the line is doubly integrated far into the wings, baseline drift and offset errors become a problem (10). Thus a good compromise appears to be the integration of lorentzian lines over the magnetic field range of $H_o - 10\Delta_o$ to $H_o + 10\Delta_o$. At these extremes, the derivative curve does not change rapidly as a function of magnetic field, so that small errors in the magnetic field limits will not affect the double integral. In order to determine the entire double integral, only a 13% correction needs to be made. This correction factor allows the instrument to be calibrated by a different material than is to be analyzed as suggested in Ref. 11, for example.

The significance of the term $\eta Q_o \chi''_{max}$ is given by several examples using the TE_{011} cavity (V_c = 56 cm^3, Q_o = 15000) and TE_{102} cavity V_c = 12.1 cm^3, Q_o = 6500) at 9.5 GHz with a sample temperature of 25 C. Using the filling factors given in Table 1, values of $4\pi\eta Q_o \chi''_{max}$ can be calculated. For example, consider a small sample of $MnSO_4 \cdot H_2O$ (12), where g = 2.00, Δ_o = 200, and θ = -26° placed at the center of the ESR cavity. If $4\pi\eta Q_o \chi''_{max}$ (Eq. 10) is to be smaller than 0.01, the sample must contain less than 3.4×10^{18} paramagnetic ions in a TE_{102} cavity, or less than 1.2×10^{18} ions in a

cavity loading parameter in Table II. A more detailed comparison is shown in Fig. 1.

The parameters that are least affected by cavity loading are Δ^2A and the doubly integrated first derivative spectrum where the limits of integration are between magnetic fields greater than about 10 times the peak-to-peak linewidth on either side of the absorption maximum. Coincidentally, relative double integrals of the spectrum recorded over a large span, such as greater than about $200\Delta_0$ on either side of the resonance field are approximately equal to relative values of Δ^2A. Apparently the increased linewidth compensates for the reduction in the peak-to-peak amplitude. Also, by computing the double integral of the first derivative spectrum far out into the wings of the line, a greater fraction of the area under the absorption that is negligibly affected by cavity loading is contributed to the analytical parameters. On the other hand, the peak-to-peak amplitude shows the greatest effect toward cavity loading. While the amplitude of the absorption would only be reduced by a factor equal to approximately $1/(4\pi\eta Q_o\chi''_{max})$, Fig. 1 shows that the peak-to-peak amplitude is reduced by a greater amount. One would initially suspect that this should not be the case, since the points of the derivative extrema occur at absorptions in which $\chi''<\chi''_{max}$. To illustrate this point, Eq. 7 can be rewritten as $F(H) = ag(H)/[1+ag(H)]$, where $g(H)$ is the lineshape function and a is a parameter proportional to $\eta Q_o\chi''_{max}$. The derivative of this function is then $dF(H)/dH = \{a/[1+ag(H)]^2\}\cdot dg(H)/dH$. Thus, where the amplitude is reduced by the factor $[1+ag(H)]^{-1}$, the derivative is reduced by $[1+ag(H)]^{-2}$. This accounts for a greater reduction for the derivative amplitude than the absorption maximum.

TE_{011} cavity. Thus, a sample of $MnSO_4 \cdot H_2O$ used as a standard should be smaller than 0.4 to 1.0 mg. depending on the cavity used. At lower temperatures the maximum sample size will be smaller since the susceptibility will increase. At higher frequencies, $\chi_o H_o$ becomes considerably greater while the cavity volume is also made smaller. This also results in a smaller sample size which can be used although this is partially compensated by lower values of Q_o.

Often the stable radical diphenylpicrylhydrazyl (DPPH) is used to calibrate ESR spectrometers. Although its lineshape is neither purely lorentzian nor gaussian, with a peak-to-peak linewidth of about 2 G, the maximum amount of sample that should be used can be estimated. For $4\pi\eta Q_o \chi'' < 0.01$, for a TE_{102} cavity the number of spins should be smaller than 3.6×10^{17}, while for a TE_{011} cavity, it should be smaller than 1.4×10^{17}. These correspond to samples of 0.1 to 0.25 mg respectively.

A final example, which pertains to the analysis of aqueous media serves to illustrate the effect of cavity loading. Typically, a flat cell of 0.05 cm^3 volume within the ESR cavity is used in a TE_{102} cavity. This arrangement reduces the Q-factor to about 2250, (13). For a sample of Mn^{2+} which exhibits a six-line spectrum with linewidth of 15 G, the concentration required to yield a value of $4\pi\eta Q_o \chi''_{max} = 0.01$ is about 0.25 M. Thus, a significant deviation of the peak-to-peak amplitude from linearity should be observed at concentrations of this order. This deviation has been observed (14). Unfortunately, because the hyperfine splitting is in the order of 85 G, there is significant overlap between adjacent lines which causes a greater value χ'' than we predict, and also because at these concentrations

electron exchange can also cause line broadening, the actual cause of the non-linearity cannot be unequivocally assigned to cavity loading effects.

Gaussian Lineshapes: A gaussian lineshape Eq.11 reflects inhomogeneous broadening of lorentzian lines

$$g(H) = \exp\left[-T_2^2(\omega-\omega_o)^2 \ln 2\right] \tag{11}$$

Since the integral of this line should equal that of the lorentzian line for a material of the same transition probability, Eq. 11 must be normalized by a factor of $(\pi \ln 2)^{\frac{1}{2}}$. Substituting relations for H and Γ, and by making use of the fact that Δ_o for a gaussian line is equal to $(2/\ln 2)^{\frac{1}{2}}\Gamma$, the microwave susceptibility is given by Eq. 12.

$$\chi'' = \left(\frac{\pi}{2}\right)^{\frac{1}{2}} \chi_o H_o \frac{1}{\Delta_o} \cdot \exp\left[-1.1768\left(\frac{H-H_o}{\Delta_o}\right)^2\right] \tag{12}$$

The value of χ''_{max} is therefore

$$\chi''_{max} = \left(\frac{\pi}{2}\right)^{\frac{1}{2}} \chi_o H_o \frac{1}{\Delta_o} \tag{13}$$

which is a factor of about 2.17 times greater than that of a lorentzian line of the same peak-to-peak width. The gaussian line is subject to less tailing than a lorenzian line, and thus virtually all of the integral of the gaussian absorption is contained within a span of about $-4\Delta_o$ to $+4\Delta_o$ from the absorption maximum. Various analytical parameters are shown as a function of $4\pi \eta Q_o \chi''_{max}$ in Fig. 2. Note here also, that the $\Delta^2 A$ is much less affected by cavity loading than is the value of A itself. This is primarily because the extent of broadening is considerably greater than for the lorentzian line.

Ferromagnetic Materials: If one assumes that a ferromagnetic material is saturated, then the susceptibility χ'' is given by Eq. 14

$$\chi'' = \mu_{eff} \beta N \, g(H) \tag{14}$$

where μ_{eff} is the effective number of Bohr magnetons per ferromagnetic atom or molecule. The function g(H) may be lorentzian. Lunar return samples, however, exhibit neither gaussian nor lorentzian lineshapes, but rather are convolutions of the lorentzian shape onto the envelope of the density of states as a function of magnetic field predicted for cubic crystalline Fe spheres (2). It is probably best to use a gaussian shape to estimate the loading factor for this case.

Integration of ESR signals. We have suggested that esr signals can be doubly integrated with precisions within $\pm$2% or better (4). The method that we used here is the following: In order to determine the baseline, the data points symmetrically disposed about the mid-point of the derivative curve are averaged. The data file is then doubly integrated after subtracting the calculated baseline from each data point. Usually the spectrum between a magnetic field range of 10 and 15 times Δ_o is used in the integration process.

Since this value is significantly different than the value of the area under the entire absorption, a correction factor is applied to the system. This factor is determined by the limits of magnetic field over which the derivative curve is integrated (1), and is given by Eq. 15

$$f = \left\{ \frac{2}{\pi} \tan^{-1}\left(\frac{H-H_o}{\Gamma}\right) - \frac{\left((H-H_o)^2/\Gamma\right)^2}{1 + \left[(H-H_o)^2/\Gamma\right]^2} \right\} \tag{15}$$

where the spectrum over the magnetic field range $H-H_o$ to H_o-H is integrated.

The value of Γ is assumed to be equal to $\sqrt{3}/2\ \Delta$.

Signals which exhibit appreciable baseline drift, are usually those recorded at high amplification. Since integration processes reduce the noise, reproducible double integral values can be obtained even with noisy derivative spectra. Although this is not the main topic of interest here, it is worth mentioning that we have found that the baseline drift is reproducible since it is most likely caused by magnetostriction of the ESR cavity. Thus, signal averaging a number of spectra of the baseline, with the cavity containing the sample holder, provides a useful signal which can be subtracted from the ESR signal of the sample. From this point, the same procedure discussed above can be used to doubly integrate the ESR signal.

A representative example of the reproducibility of the double integration process is in the six repetitions of a 1.5 mg sample of $MnSO_4 \cdot H_2O$. The sample was left at the same instrumental parameters so that other uncertainties, eg. positioning, setting the power level, and changing the field sweep rate do not affect the result. The peak-to-peak amplitude agreed to within ± 1 bit of the A to D converter (0.02%) and the standard deviation of the double integral processing where the field between H_o-20Γ and H_o+20Γ was utilized was 0.9%. A smaller standard deviation was obtained when the integration limits were reduced to H_o-10Γ to H_o+10Γ.

Experimental Verification. In order to confirm the calculations presented here, samples of $MnSO_4 \cdot H_2O$ weighing between 1.5 and 105 mg. were recorded. The filling factors of each sample were calculated from the equation (4)

$$\kappa = \frac{1}{2}\left[1 + \frac{L}{\pi l_s} \sin\left(\frac{\pi l_s}{L}\right)\right]$$

where L is the length of the cavity (2.24 cm) and l_s is the length of the sample in the 3mm id quartz tube. Since a TE_{104} cavity was used here rather than the TE_{102} cavity described earlier, the factor of 1/2 corrects for the cavity volume so that V_c remains 12.0 cm^3. The longest sample used here was 1.8 cm which has a value of κ equal to 0.62. Note that in a TE_{104} cavity twice as much material is required to degrade the Q-factor by the same amount as a TE_{102} cavity.

Double integrals, peak-to-peak amplitudes, and peak-to-peak linewidths are shown in Fig. 3. The bold curves are derived from the calculated values for $MnSO_4 \cdot H_2O$ in the previous sections, and from the data in Table I. The experiments show remarkable agreement with the theory considering that there are no adjustable parameters, and the perturbation of the microwave field due to the sample dielectric or absorption is not taken into account.

Significant degradation of the cavity Q-factor for samples of 25 mg or more can be seen from the oscilloscope trace of the cavity mode as the magnetic field is passed through resonance. This permits a crude approximation of the change in cavity Q on and off resonance. For example, cavity Q-factors with the sample containing 47 mg and κ = 0.90, were measured. Assuming that the maximum of the klystron mode corresponded to the total reflected power, the half width of the cavity mode was measured at zero field, and at the resonance maximum, and the microwave frequency was calibrated with a wavemeter. The value of Q_0 was estimated to be 6700 ± 300, while Q at resonance was 5400 ± 250. The value of $\Delta Q/Q_0$ is therefore 0.19 ± 0.08. From the previous calculation, a sample of 1.88 mg at η = 1 should cause a value of $\Delta Q/Q$ of 0.01. Thus for the 47 mg sample, $\Delta Q/Q$ is predicted to

be about 0.23, in agreement with the estimated value.

CONCLUSIONS

Sample size is a critical parameter in analytical determinations utilizing electron spin resonance spectroscopy, due to effects on cavity loading during the resonance absorption. The maximum sample size which can be used depends upon the magnetic parameters of the material and the cavity and sample geometries. Parameters least affected by loading are the double integral and the peak-to-peak amplitude times the square of the linewidth. The peak-to-peak amplitude is most greatly affected. While the linewidth of the sample is subject to poor accuracy, the double integral of the first derivative spectrum can be obtained with precisions of better than $\pm$1% in many cases by using digital recording and data processing.

ACKNOWLEDGEMENTS

Helpful discussions with Robert M. Housley are gratefully acknowledged.

This work was supported by the Office of Naval Research.

LITERATURE CITED

1. I. B. Goldberg and A. J. Bard, "Analytical Applications of Electron Spin Resonance" in I. M. Kollhoff, P. J. Elving, and M. M. Bursey, eds. Treatise on Analytical Chemistry, 2nd ed. Pt. 1, V. 6, in press: Science Center Manuscript SCM-76-125.
2. R. M. Housley, E. H. Cirlin, I. B. Goldberg, and H. R. Crowe, Proceedings of the 7th Lunar Science Conference, Houston, Texas, Vol. 1, p.23, 1976.
3. A. A. Westenberg, Progr. Reaction Kinetics 7, pt. 1, 23 (1973).
4. I. B. Goldberg, H. R. Crowe, and W. M. Robertson, Anal. Chem., submitted.
5. G. Feher, Bell Sys. Tech. J., 36, 449 (1957).
6. B. Vigouroux, J. C. Gourdon, P. Lopez, and J. Pescia, J. Phys. E, 6, 557 (1973).
7. I. B. Goldberg, H. R. Crowe, and R. S. Carpenter, J. Magn. Reson., 18, 84 (1975).
8. C. P. Poole "Electron Spin Resonance" Interscience, N. Y. 1967. Chapters 8 and 14.
9. G. E. Pake, "Paramagnetic Resonance", W. A. Benjamin, N. Y. 1962, pp. 21-30.
10. M. L. Randolph, "Quantitative Considerations in Electron Spin Resonance of Biological Materials", in H. M. Swartz, J. R. Bolton, and D. C. Borg, eds. Biological Applications of Electron Spin Resonance, John W. N. Y., 1972. Chapter 3.
11. J. R. Bolton, D. C. Borg, and H. M. Swartz, "Experimental Aspects of Biological Electron Spin Resonance Studies", in H. M. Swartz,

J. R. Bolton, and D. C. Borg, eds, "Biological Applications of Electron Spin Resonance, John Wiley, N. Y., 1972. Chapter 2.

12. Y. Allain, J. P. Krebs, and J. de Gunzbourg, J. Appl. Phys., 39, 1124 (1968).

13. Varian Aqueous Sample Cell Instruction Manual.

14. G. G. Guilbault and G. J. Lubrano, Anal. Lett., 1, 725 (1968).

TABLE I

Typical Filling Factors*

	η	η if $2a = d$
TE_{011} (Cylindrical)		
small sample at cavity center	$\frac{12.33}{1 + \left(\frac{0.82a}{d}\right)^2} \cdot \frac{V_s}{V_c}$	$10.56 \frac{V_s}{V_c}$
tube of radius r R along cavity axis	$\frac{6.16}{1 + \left(\frac{0.82a}{d}\right)^2} \cdot \frac{V_s}{V_c}$	$5.27 \frac{r^2}{R^2}$
TE_{102} (rectangular)		
small sample of cavity center	$\frac{4}{1 + \left(\frac{d}{2a}\right)^2} \cdot \frac{V_s}{V_c}$	$2.00 \frac{V_s}{V_c}$
tube of radius r along sample axis	$\frac{2}{1 + \left(\frac{d}{2a}\right)^2} \cdot \frac{V_s}{V_c}$ (if r a)	$1.00 \frac{\pi r^2}{b\ d}$
flat cell of thickness d' and width b'	$\frac{2}{1 + \left(\frac{d}{2a}\right)^2} \cdot \frac{V_s}{V_c}$	$1.00 \frac{b'd'}{b\ d}$
special case Varian TE_{01n} with 2.17 cm i.d. quartz tube		0.331

V_c = cavity volume; V_s = sample volume
cylindrical cavity: a = radius; d = length
rectangular cavity: a = thickness; b = width (parallel to static field); d = length.

TABLE II

Relative Peak-to-Peak Linewidths, Amplitudes and Double Integrals for Various Cavity Loading Parameters to that in the absence of loading for a Lorentzian Line

Parameter $(4\pi\eta\chi''_{max}Q_o)$	Peak-to-Peak Width (Δ/Δ_o)	Amplitude (A/A_o)	Double Integral Limit
0.000	1.000	1.0000	1.0000
0.001	1.000	0.9988	0.9995
0.002	1.000	0.9972	0.9990
0.005	1.001	0.9928	0.9975
0.010	1.003	0.9854	0.9950
0.020	1.009	0.9709	0.9901
0.050	1.026	0.9296	0.9759
0.080	1.032	0.8912	0.9622
0.100	1.046	0.8669	0.9534
0.150	1.064	0.8111	0.9325
0.200	1.087	0.7609	0.9129
0.350	1.153	0.6377	0.8606
0.500	1.210	0.5444	0.8165
0.800	1.347	0.4142	0.7454
1.000	1.416	0.3537	0.7071
1.500	1.565	0.2530	0.6324
2.000	1.722	0.1925	0.5774
3.500	2.094	0.1048	0.4713
5.000	2.430	0.0681	0.4082
8.000	2.981	0.0371	0.3333
10.000	3.277	0.0275	0.3015

FIGURE CAPTIONS

Fig. 1: Plot of the relative peak-to-peak amplitude, peak-to-peak amplitude multiplied by the square of the linewidth, and double integrals over different magnetic field regions against the cavity loading parameter 4 Q_0 χ''_{max}. The parameter $(1-4\ Q_0\ \chi''_{max})^{-1}$ is included for reference. Values of the relative parameter less than unity reflect deviations from linearity in the particular ESR signal vs. concentration or quantity of material.

Fig. 2: Plot of the relative peak-to-peak amplitude, double integral, and peak-to-peak amplitude multiplied by the square of the linewidth. Deviations from unity in the relative values reflect a non-linearity if the ESR signal vs. concentration or quantity of material.

Fig. 3: Double integral recorded over the field range H_0-20 to H_0 + 20 , peak-to-peak amplitude, and peak-to-peak linewidth of the derivative ESR signal for $MnSO_4 \cdot H_2O$ vs. the filling factor times the weight of the sample in a TE_{104} cavity. Curves show the theoretical values based on the parameters: Q_0 = 6500; ν = 9.50 GHz; θ = -26°K; T = 300°K, g = 2.00; Δ_0 = 200.G; S = 5/2. Samples are weighed to $\pm$0.05 mg. Incident microwave power: ● 0.82 mW; ■, 2.46 mW; 0, 25.0 mW.

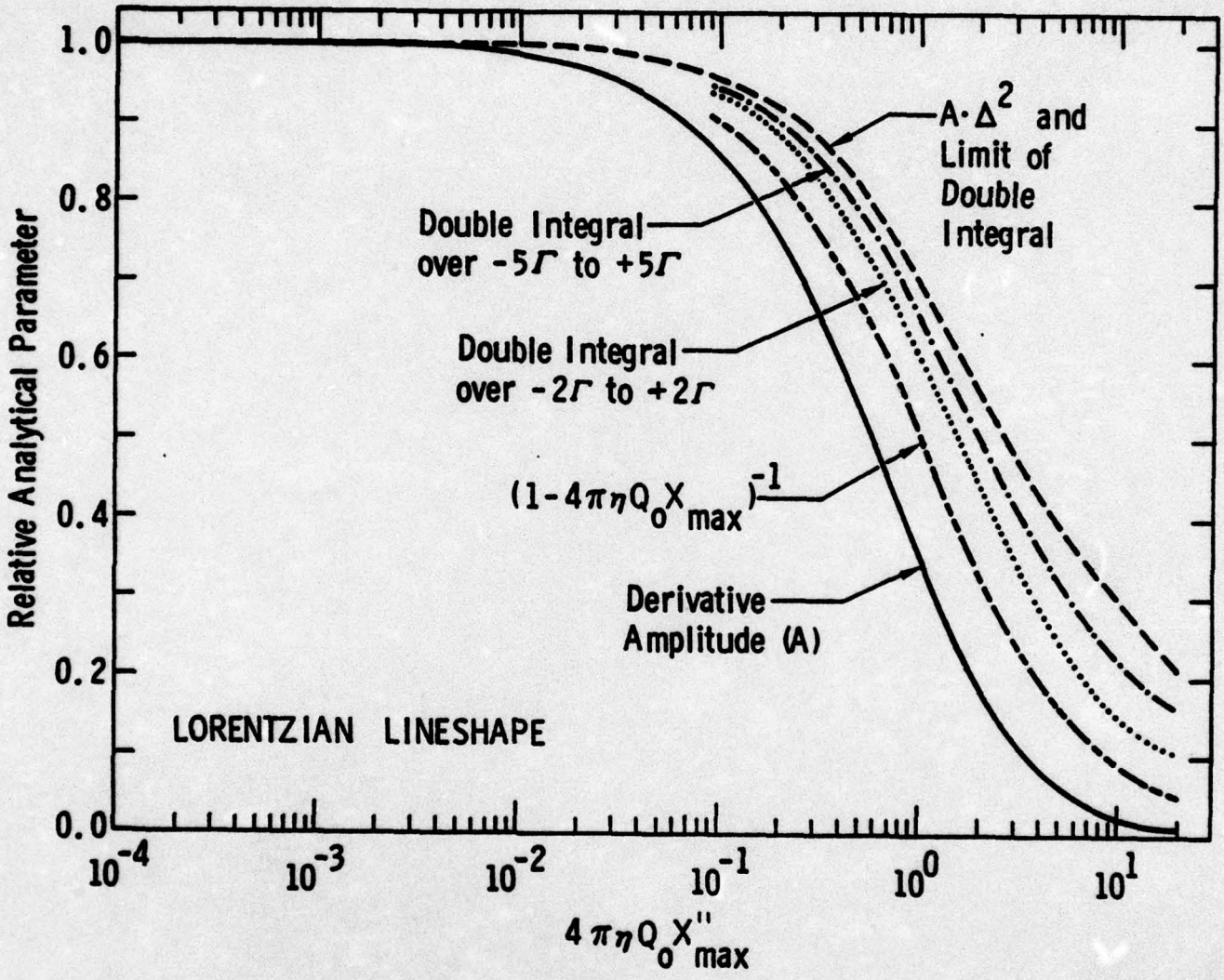
1.0
0.8
0.6
0.4
0.2
0.0
Relative Analytical Parameter
$A \cdot \Delta^2$ and Limit of Double Integral
Double Integral over -5Γ to $+5\Gamma$
Double Integral over -2Γ to $+2\Gamma$
$(1-4\pi\eta Q_o X_{max})^{-1}$
Derivative Amplitude (A)
LORENTZIAN LINESHAPE
10^{-4}
10^{-3}
10^{-2}
10^{-1}
10^{0}
10^{1}
$4\pi\eta Q_o X''_{max}$

Fig. 1

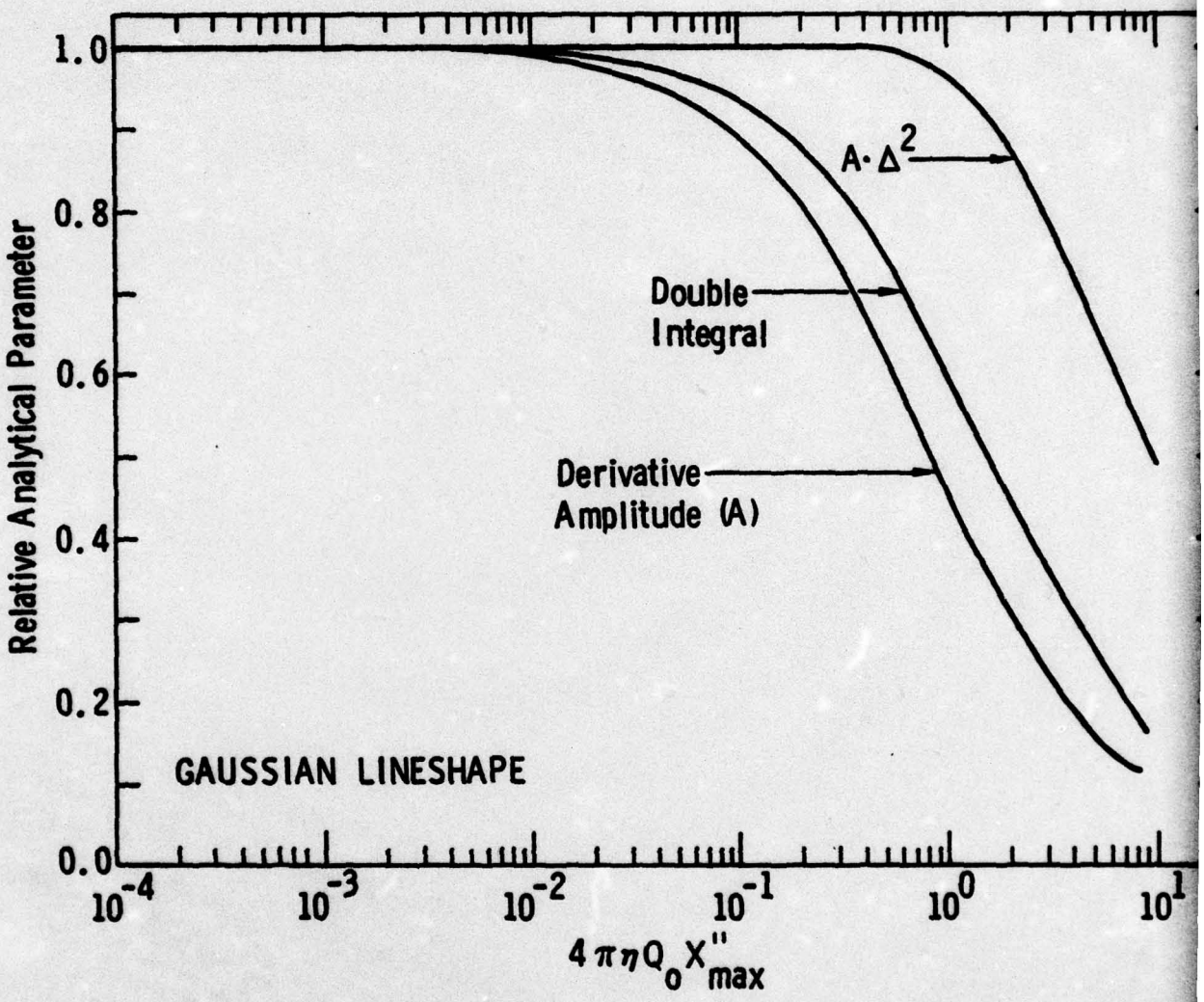
1.0
0.8
0.6
0.4
0.2
0.0
Relative Analytical Parameter
A·Δ²
Double
Integral
Derivative
Amplitude (A)
GAUSSIAN LINESHAPE
10⁻⁴
10⁻³
10⁻²
10⁻¹
10⁰
10¹
4πηQ₀X''max

Fig. 2

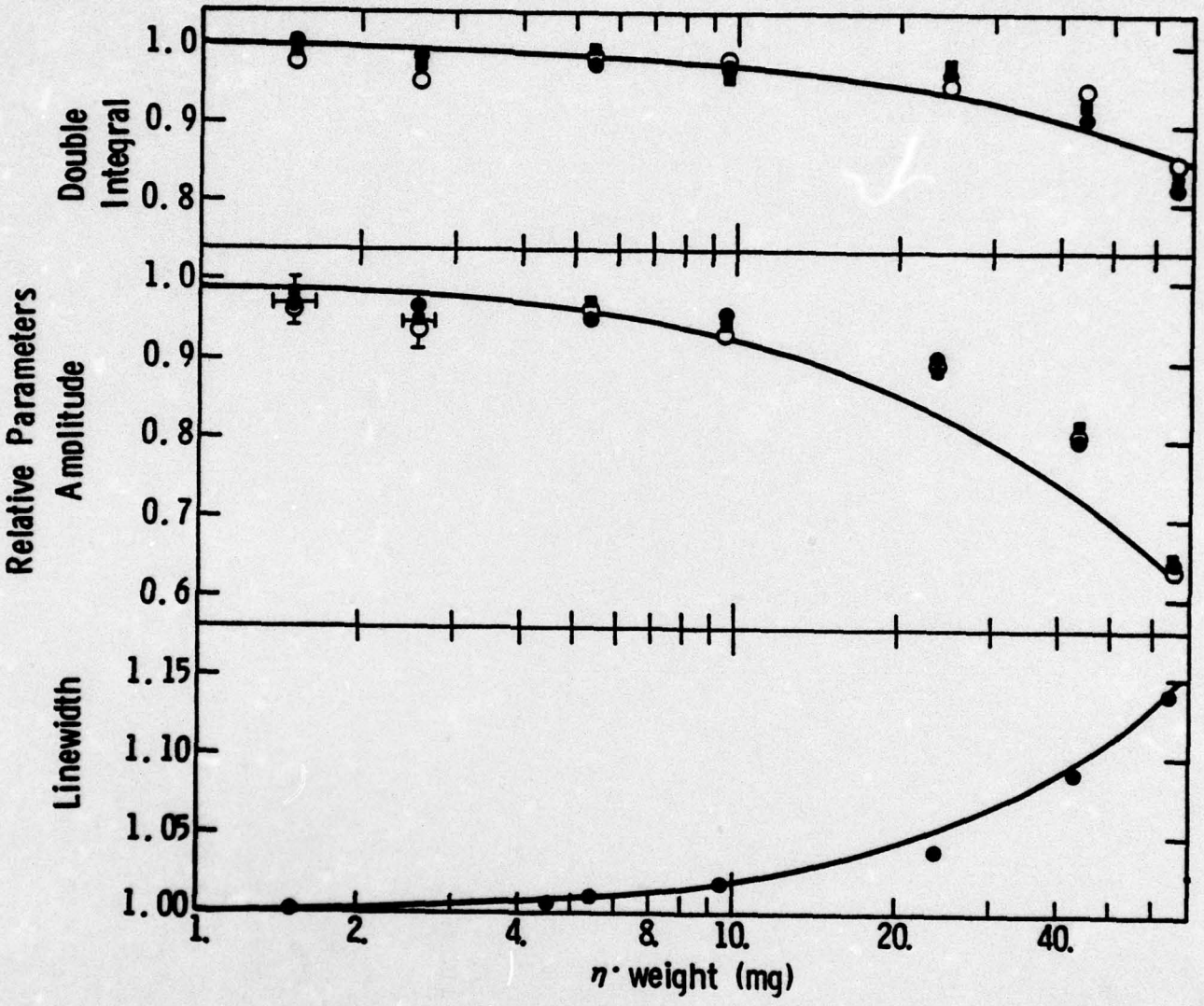
Relative Parameters
Double Integral
Amplitude
Linewidth
1.0
0.9
0.8
0.7
0.6
1.15
1.10
1.05
1.00
1.
2.
4.
8.
10.
20.
40.
η · weight (mg)

Fig. 3

TECHNICAL REPORT DISTRIBUTION LIST

	No. Copies
Office of Naval Research Arlington, Virginia 22217 Attn: Code 472	2
Office of Naval Research Arlington, Virginia 22217 Attn: Code 102IP	6
ONR Branch Office 536 S. Clark Street Chicago, Illinois 60605 Attn: Dr. George Sandoz	1
ONR Branch Office 715 Broadway New York, New York 10003 Attn: Scientific Dept.	1
ONR Branch Office 1030 East Green Street Pasadena, California 91106 Attn: Dr. R. J. Marcus	1
ONR Branch Office 760 Market Street, Rm. 447 San Francisco, California 94102 Attn: Dr. P. A. Miller	1
ONR Branch Office 495 Summer Street Boston, Massachusetts 02210 Attn: Dr. L. H. Peebles	1
Director, Naval Research Laboratory Washington, D.C. 20390 Attn: Library, Code 2029 (ONRL) Technical Info. Div. Code 6100, 6170	6 1 1
The Asst. Secretary of the Navy (R&D) Department of the Navy Room 4E736, Pentagon Washington, D.C. 20350	1
Commander, Naval Air Systems Command Department of the Navy Washington, D.C. 20360 Attn: Code 310C (H. Rosenwasser)	1

	No.
Defense Documentation Center Building 5, Cameron Station Alexandria, Virginia 22314	1
U.S. Army Research Office P.O. Box 12211 Research Triangle Park, North Carolina 27 Attn: CRD-AA-IP	1
Commander Naval Undersea Research & Development Center San Diego, California 92132 Attn: Technical Library, Code 133	1
Naval Weapons Center China Lake, California 93555 Attn: Head, Chemistry Division	1
Naval Civil Engineering Laboratory Port Hueneme, California 93041 Attn: Mr. W. S. Haynes	1
Professor O. Heinz Department of Physics & Chemistry Naval Postgraduate School Monterey, California 93940	1
Dr. A. L. Slafkosky Scientific Advisor Commandant of the Marine Corps (Code RD-1) Washington, D.C. 20380	1

TECHNICAL REPORT DISTRIBUTION LIST

	No. Copies
Dr. M. B. Denton University of Arizona Department of Chemistry Tucson, Arizona 85721	1
Dr. G. S. Wilson University of Arizona Department of Chemistry Tucson, Arizona 85721	1
Dr. R. A. Osteryoung Colorado State University Department of Chemistry Fort Collins, Colorado 80521	1
Dr. B. R. Kowalski University of Washington Department of Chemistry Seattle, Washington 98105	1
~~Dr. I. B. Goldberg~~ ~~North American Rockwell Science Center~~ ~~P.O. Box 1085~~ ~~1049 Camino Dos Rios~~ ~~Thousand Oaks, California 91360~~	~~1~~
Dr. S. P. Perone Purdue University Department of Chemistry Lafayette, Indiana 47907	1
Dr. E. E. Wells Naval Research Laboratory Code 6160 Washington, D.C. 20375	1
Dr. D. L. Venezky Naval Research Laboratory Code 6130 Washington, D.C. 20375	1
Dr. H. Freiser University of Arizona Department of Chemistry Tucson, Arizona 85721	1

	No. Copies
Dr. Fred Saalfeld Naval Research Laboratory Code 6110 Washington, D.C. 20375	1
Dr. H. Chernoff Massachusetts Institute of Technology Department of Mathematics Cambridge, Massachusetts 02139	1
Dr. K. Wilson University of California, San Diego Department of Chemistry La Jolla, California 92037	1
Dr. A. Zirino Naval Undersea Center San Diego, California 92132	1
Dr. John Duffin United States Naval Post Graduate School Monterey, California 93940	1
Dr. G. M. Hieftje Department of Chemistry Indiana University Bloomington, Indiana 47401	1
Dr. Victor L. Rehn Naval Weapons Center Code China Lake, California 93555	1